A First Step of Humanoid's Walking by Two Degree-of-freedom Generalized Predictive Control Combined with Visual Lifting Stabilization

Akira Yanou, Mamoru Minami, Tomohide Maeba and Yosuke Kobayashi
Graduate School of Natural Science and Technology
Okayama University
Okayama, Japan 700–8530
Email: {yanou, minami, maeba, kobayashi2}@suri.sys.okayama-u.ac.jp

***Abstract*—Biped locomotion created by a controller based on Zero-Moment Point (ZMP) known as reliable control method looks different from human's walking on the view point that ZMP-based walking does not include falling state. However, the walking control that does not depend on ZMP is vulnerable to turnover. Therefore, keeping the walking of dynamical motion stable is inevitable issue for realization of human-like natural walking—we call the humans' walking that includes turning over states as "natural." In our research group, walking model including slipping, impact, surface-contacting and point-contacting of foot has been developed. Although "Visual Lifting Stabilization" (VLS) strategy has been also proposed in order to enhance standing robustness and prevent the robot from falling down without utilizing ZMP, the torque generation strategy making lifted-leg step forward is derived by trial and error. Therefore, as a first step to realize humans' walking, this paper explores two degree-of-freedom generalized predictive control (GPC) method in order to generate the torque making lifted-leg step forward. Simulation results indicate that this strategy helps stabilize bipedal walking even though ZMP is not kept inside convex hull of supporting area.**

I. Introduction

Avoiding complications in dealing directly with true dynamics of humanoid without approximation, inverted pendulum has been used frequently for making a stable controller [1], [2], [3] for realizing stable walking, simplifying the calculations for controller. Further, linear approximation having the humanoid changed into simple inverted pendulum enables researchers to realize stable gait through well-known control strategy [4], [5]. As for walking control of the humanoid, ZMP-based walking is known as the most potential approach, which has been proved to be a realistic control strategy to demonstrate stable walking of actual biped robots, since it can guarantee that the robots can keep standing by retaining the ZMP within the convex hull of supporting area [6], [7]. Instead of the ZMP, there are another approaches that put the importance on keeping the robot's walking trajectories inside of a basin of attraction [8], [9] including a method referring limit cycle to determine input torque [10].

These previous discussions are based on simplified bipedal models, which tend to avoid discussing the effects of feet or slipping existing in real world. Contrarily to the above references, a research [11] has pointed out that the effect of foot bears varieties of the walking gait. Our research has begun from such view point of [11] and been developedas aiming at describing gait's dynamics as correctly as possible, including surface/point-contacting state of foot and toe, slipping of the foot and impact, where walking gait states transfer based on the walking motions results, called event-driven. However, our model differs from [11] in that it uses leg model without body, arms and head, instead of that we discuss the dynamics of whole-body humanoid. And that what our research group thinks important is that the dimension of dynamical equation will change depending on the walking gait's varieties, which introduced by [12] concerning one-legged hopping robot. Given as an example that heel be detached from ground while its toe being contacting, a new state variable describing foot's rotation would emerge, resulting in an increase of a number of state variables. Further the tipping over motion has been called as non-holonomic dynamics that includes a joint without inputting torque, i.e., free joint. Meanwhile, landing of the heel or the toe of lifting leg in the air to the ground makes a geometrical contact. Reference [13] mentioned how to represent contacting with environment that can handle constraint motion with friction by algebraic equation and applied it to human figures. We derive dynamics of eleven kinds of gaits based on these references, where our belief that making the humanoid's dynamical model elaborate as much as possible leads the simulation to be realistic underlies.

When ZMP is to be on the edge of convex hull of foot, meaning the humanoid is in a state of tipping over, the gait deems to be unstable. In our research group, ZMP-independent walking method has been proposed to realize human-like natural walking including tipping over state, that is a method to enhance standing robustness named "Visual Lifting Stabilization" (VLS) strategy [14] based on visual servoing and visual feedback concept, which is based on a similar concept of impedance control method [15]. But the torque generation strategy making lifted-leg step forward is derived by trial and error. For this trial and error, we believe that the concept of prediction is effective in torque generation strategy similar to humans' walking. Therefore, as a first step to realize humans' walking, this paper explores two degree-of-freedom generalized predictive control (GPC) method [16] in order to generate the torque making lifted-leg step forward. The simulation results show that two degree-of-freedom GPC combined with VLS helps realize stable bipedal walking that ZMP is not kept within convex hull of supporting area on

978-1-4799-0224-8/13/$31.00 ©2013 IEEE

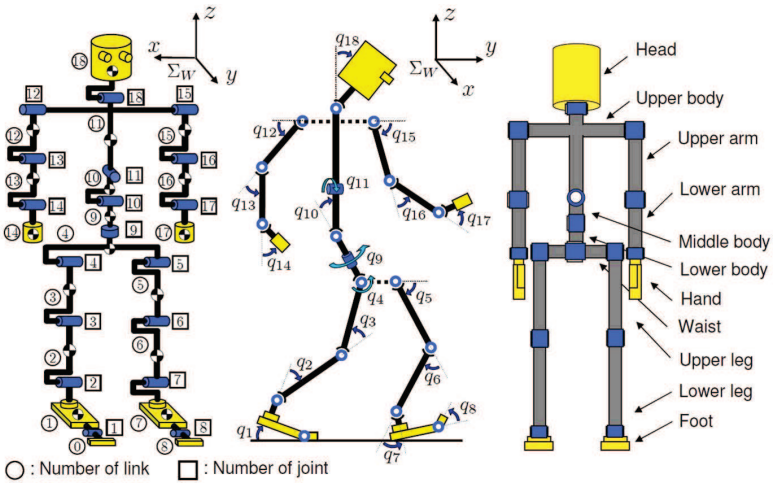

Fig. 1. Definition of humanoid's link, joint and angle number

TABLE I. PHYSICAL PARAMETERS

Link	l_i	m_i	d_i
Head	0.24	4.5	0.5
Upper body	0.41	21.5	10.0
Middle body	0.1	2.0	10.0
Lower body	0.1	2.0	10.0
Upper arm	0.31	2.3	0.03
Lower arm	0.24	1.4	1.0
Hand	0.18	0.4	2.0
Waist	0.27	2.0	10.0
Upper leg	0.38	7.3	10.0
Lower leg	0.40	3.4	10.0
Foot	0.07	1.1	10.0
Total	1.7	63.8	

condition that humanoid's dynamics includes tipping, slipping and impact.

II. DYNAMICAL WALKING MODEL

We discuss a biped robot whose definition is depicted in Fig. 1. Table I indicates length l_i [m], mass m_i [kg] of links and joints' coefficient of viscous friction d_i [N·m·s/rad], which are decided based on [17]. Like reference [18]—it includes no ramifications—we derive the dynamics of humanoid being simulated as a serial-link manipulator having ramifications by Newton-Euler formulation [19]. Our model represents rigid whole body—feet including toe, torso, arms and body—having 18 degree-of-freedom. Though motion of legs is restricted in sagittal plane, it generates varieties of walking gait sequences since the robot has flat-sole feet and kicking torque. In this paper, one foot including link-0 (tiptoe) and link-1 (foot) is defined as "supporting-foot" and the other foot including link-7 and link-8 is named as "floating-foot" or "contacting-foot."

A. Model of Single-foot Standing

We get equation of motion with one leg standing as:

$$\boldsymbol{M}(\boldsymbol{q})\ddot{\boldsymbol{q}} + \boldsymbol{h}(\boldsymbol{q}, \dot{\boldsymbol{q}}) + \boldsymbol{g}(\boldsymbol{q}) + \boldsymbol{D}\dot{\boldsymbol{q}} = \boldsymbol{\tau}, \tag{1}$$

where, $\boldsymbol{M}(\boldsymbol{q})$ is inertia matrix, $\boldsymbol{h}(\boldsymbol{q}, \dot{\boldsymbol{q}})$ and $\boldsymbol{g}(\boldsymbol{q})$ are vectors which indicate Coriolis force, centrifugal force and gravity, $\boldsymbol{D} = \mathrm{diag}\{d_1, d_2, \cdots, d_{18}\}$ is matrix which means coefficients of joints' viscous friction and $\boldsymbol{\tau}$ is input torque. If supporting-foot is surface-contacting and assumed to be without slipping, joint angles can be thought as $\boldsymbol{q} = [q_2, q_3, \cdots, q_{18}]^{\mathrm{T}}$. This walking pattern is depicted in Fig. 2 (a). When heel of supporting-foot should detach from the ground before floating-foot contacts to the ground as shown in Fig. 2 (b), the state variable for the foot's angle q_1 be added to $\boldsymbol{q}$, thus $\boldsymbol{q} = [q_1, q_2, \cdots, q_{18}]^{\mathrm{T}}$. In this state, input torque τ_1 for toe is set as always to be zero, i.e., non-holonomic and tipping over state.

B. Model with Contacting Constraints

Giving that floating-foot contacts with a ground, two possible states like Fig. 3 appear, where contacting-foot's position

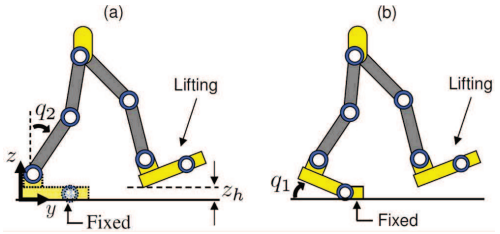

Fig. 2. Gaits including floating-foot

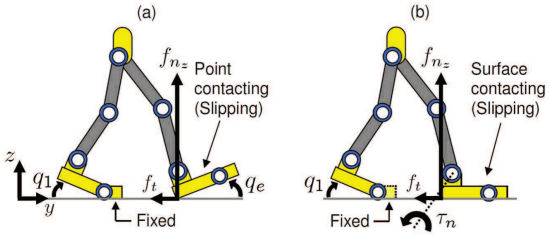

Fig. 3. Gaits including contacting-foot (Slipping)

z_h or angle q_e to the ground are constrained. In Fig. 3 (a) and (b), since the foot is constrained only vertical direction, foot's motion in walking direction (y-axis) has a degree of motion, that is, contacting-foot may slip forward or backward depending on the foot's velocity when contacting happens. Given that constraints of foot's position and foot's rotation are defined as C_1 and C_2 respectively, these constraints are represented by Eq. (2), where $\boldsymbol{r}(\boldsymbol{q})$ means the contacting-foot's heel or toe position.

$$\boldsymbol{C}(\boldsymbol{r}(\boldsymbol{q})) = \begin{bmatrix} C_1(\boldsymbol{r}(\boldsymbol{q})) \\ C_2(\boldsymbol{r}(\boldsymbol{q})) \\ C_3(\boldsymbol{r}(\boldsymbol{q})) \end{bmatrix} = \boldsymbol{0} \tag{2}$$

Here, C_3 is the constraint that contacting-foot does not slip (y_h is constant) as shown in Fig. 4, which appears when velocity of the foot $\dot{y}_h$ in walking direction becomes less than small constant value ε in case of $|\dot{y}_h| < \varepsilon$, meaning dynamic friction changes to static friction. On the other hand, C_3 disappears when contacting-foot's force f_y in walking direction exceeds

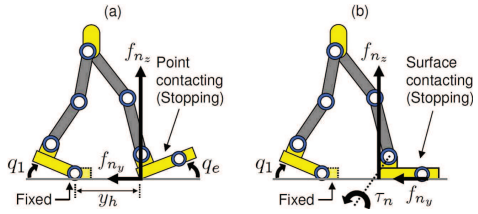

Fig. 4. Gaits including contacting-foot (No slipping)

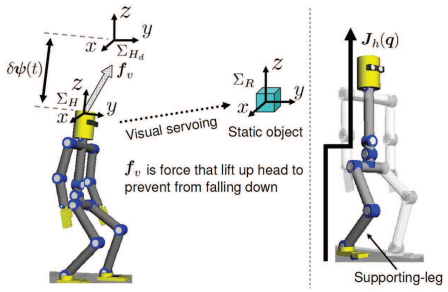

Fig. 5. Concept of Visual Lifting Stabilization

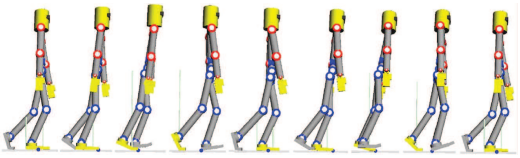

Fig. 6. Screen-shot of bipedal walking

friction force f_t in case of $|f_y| > |f_t|$, meaning static friction changes to dynamic friction and slipping begins. Then, robot's equation of motion with external force f_{n_z}, f_{n_y}, friction force f_t and external torque τ_n corresponding to C_1, C_2 and C_3 can be derived as follows:

$$\boldsymbol{M}(\boldsymbol{q})\ddot{\boldsymbol{q}} + \boldsymbol{h}(\boldsymbol{q},\dot{\boldsymbol{q}}) + \boldsymbol{g}(\boldsymbol{q}) + \boldsymbol{D}\dot{\boldsymbol{q}} = \boldsymbol{\tau} + \boldsymbol{j}_{c_z}^{\mathrm{T}} f_{n_z} - \boldsymbol{j}_t^{\mathrm{T}} f_t + \boldsymbol{j}_r^{\mathrm{T}} \tau_n + \boldsymbol{j}_{c_y}^{\mathrm{T}} f_{n_y}, \quad (3)$$

where $\boldsymbol{j}_{c_z}$, $\boldsymbol{j}_t$, $\boldsymbol{j}_r$ and $\boldsymbol{j}_{c_y}$ are defined as:

$$\boldsymbol{j}_{c_z}^{\mathrm{T}} = \left(\frac{\partial C_1}{\partial \boldsymbol{q}^{\mathrm{T}}}\right)^T \left(1/\left\|\frac{\partial C_1}{\partial \boldsymbol{r}^{\mathrm{T}}}\right\|\right), \quad \boldsymbol{j}_t^{\mathrm{T}} = \left(\frac{\partial \boldsymbol{r}}{\partial \boldsymbol{q}^{\mathrm{T}}}\right)^T \frac{\dot{\boldsymbol{r}}}{\|\dot{\boldsymbol{r}}\|},$$
$$\boldsymbol{j}_r^{\mathrm{T}} = \left(\frac{\partial C_2}{\partial \boldsymbol{q}^{\mathrm{T}}}\right)^{\mathrm{T}} \left(1/\left\|\frac{\partial C_2}{\partial \boldsymbol{q}^{\mathrm{T}}}\right\|\right), \quad \boldsymbol{j}_{c_y}^{\mathrm{T}} = \left(\frac{\partial C_3}{\partial \boldsymbol{q}^{\mathrm{T}}}\right)^{\mathrm{T}} \left(1/\left\|\frac{\partial C_3}{\partial \boldsymbol{r}^{\mathrm{T}}}\right\|\right).$$

It is common sense that (i) f_{n_z} (constraint force normal to floor) and f_t (friction force tangential to floor surface) are orthogonal, and (ii) value of f_t depends on f_{n_z} as $f_t = K f_{n_z}$ (K is constant scalar: $0 < K \leq 1$).

Moreover, differentiating Eq. (2) by time two times, then we can derive the constraint condition of $\ddot{\boldsymbol{q}}$.

$$\left(\frac{\partial C_i}{\partial \boldsymbol{q}^{\mathrm{T}}}\right)\ddot{\boldsymbol{q}} + \dot{\boldsymbol{q}}^{\mathrm{T}} \left\{\frac{\partial}{\partial \boldsymbol{q}}\left(\frac{\partial C_i}{\partial \boldsymbol{q}^{\mathrm{T}}}\right)\right\}\dot{\boldsymbol{q}} = 0 \quad (i = 1,2,3) \quad (4)$$

Should the $\ddot{\boldsymbol{q}}$ in Eqs. (3), (4) be identical so the time solution of Eq. (4) be under the constraint of Eq. (2), then the following simultaneous equation of $\ddot{\boldsymbol{q}}$, f_{n_z}, τ_n and f_{n_y} have to be maintained during the contacting motion [13]. Here, f_{n_z}, τ_n and f_{n_y} are decided dependently to make the $\ddot{\boldsymbol{q}}$ in Eqs. (3), (4) be identical.

$$\begin{bmatrix} \boldsymbol{M}(\boldsymbol{q}) & -(\boldsymbol{j}_{c_z}^T - \boldsymbol{j}_t^T K) & -\boldsymbol{j}_r^T & -\boldsymbol{j}_{c_y}^T \\ \partial C_1/\partial \boldsymbol{q}^{\mathrm{T}} & 0 & 0 & 0 \\ \partial C_2/\partial \boldsymbol{q}^{\mathrm{T}} & 0 & 0 & 0 \\ \partial C_3/\partial \boldsymbol{q}^{\mathrm{T}} & 0 & 0 & 0 \end{bmatrix} \begin{bmatrix} \ddot{\boldsymbol{q}} \\ f_{n_z} \\ \tau_n \\ f_{n_y} \end{bmatrix}$$
$$= \begin{bmatrix} \boldsymbol{\tau} - \boldsymbol{h}(\boldsymbol{q},\dot{\boldsymbol{q}}) - \boldsymbol{g}(\boldsymbol{q}) - \boldsymbol{D}\dot{\boldsymbol{q}} \\ -\dot{\boldsymbol{q}}^{\mathrm{T}} \left\{\frac{\partial}{\partial \boldsymbol{q}}\left(\frac{\partial C_1}{\partial \boldsymbol{q}^{\mathrm{T}}}\right)\right\}\dot{\boldsymbol{q}} \\ -\dot{\boldsymbol{q}}^{\mathrm{T}} \left\{\frac{\partial}{\partial \boldsymbol{q}}\left(\frac{\partial C_2}{\partial \boldsymbol{q}^{\mathrm{T}}}\right)\right\}\dot{\boldsymbol{q}} \\ -\dot{\boldsymbol{q}}^{\mathrm{T}} \left\{\frac{\partial}{\partial \boldsymbol{q}}\left(\frac{\partial C_3}{\partial \boldsymbol{q}^{\mathrm{T}}}\right)\right\}\dot{\boldsymbol{q}} \end{bmatrix} \quad (5)$$

As shown in Figs. 2–4, contacting patterns make the dimension of state variables change and they change constraint conditions vice versa.

III. Bipedal Walking Strategy

A. Visual Lifting Stabilization

This section describes a vision-feedback control for improving humanoid's standing/walking stability as shown in Fig. 5. We use a model-based matching method to measure pose of a static target object denoted by $\boldsymbol{\psi}(t)$ based on Σ_H, which represents the robot's head. The desired relative pose of Σ_R (reference target object's coordinate) and Σ_H is predefined by Homogeneous Transformation as ${}^H\boldsymbol{T}_R$. The difference between the desired head pose Σ_{H_d} and the current pose Σ_H is denoted as ${}^H\boldsymbol{T}_{H_d}$, it can be described by:

$${}^H\boldsymbol{T}_{H_d}(\boldsymbol{\psi}_d(t), \boldsymbol{\psi}(t)) = {}^H\boldsymbol{T}_R(\boldsymbol{\psi}(t)) \cdot {}^{H_d}\boldsymbol{T}_R{}^{-1}(\boldsymbol{\psi}_d(t)), \quad (6)$$

where, although ${}^H\boldsymbol{T}_R$ is calculated by $\boldsymbol{\psi}(t)$ that can measured by on-line visual pose estimation method [20], we assume this parameter as being detected correctly in this paper. Here, the force exerted on the head to minimize $\delta\boldsymbol{\psi}(t) = \boldsymbol{\psi}_d(t) - \boldsymbol{\psi}(t)$ calculated from ${}^H\boldsymbol{T}_{H_d}$—the pose deviation of the robot's head caused by gravity force and walking dynamical influences—is considered to be directly proportional to $\delta\boldsymbol{\psi}(t)$. The joint torque $\boldsymbol{\tau}_h(t)$ that pulls the robot's head up is given the following equation:

$$\boldsymbol{\tau}_h(t) = \boldsymbol{J}_h(\boldsymbol{q})^{\mathrm{T}} \boldsymbol{K}_p \delta\boldsymbol{\psi}(t), \quad (7)$$

where $\boldsymbol{J}_h(\boldsymbol{q})$ in Fig. 5 is Jacobian matrix of the head pose against joint angles including $q_1, q_2, q_3, q_4, q_9, q_{10}, q_{11}, q_{18}$, and $\boldsymbol{K}_p$ means proportional gain similar to impedance control. We use this input to compensate the falling motions caused by gravity or dangerous slipping motion happened unpredictably during walking states [21]. Notice that the input torque for non-holonomic joint like joint-1 (toe of supporting-foot), τ_{h_1} in $\boldsymbol{\tau}_h(t)$ in Eq. (7) is to be set as zero since it is free joint. Although $\delta\boldsymbol{\psi}(t)$ can represent error concerning the humanoid's both position and orientation, only position was utilized in this research, so $\boldsymbol{K}_p$ was set as $\boldsymbol{K}_p = \mathrm{diag}\{20, 290, 1100\}^{\mathrm{T}}$.

B. Two degree-of-freedom GPC as lifted-leg motion generator

Generalized predictive control (GPC) was proposed by Clarke and others in 1987 [22] and has been widely applied

in industry. The control law is derived by minimization of a performance index, which includes an error between reference signal and controlled output and a control input. And the controlled output can track a step-type reference signal robustly because the integral compensation embedded in the controller always acts. However, its integral compensation may cause slow transient response or extra control input. On the other hand the authors have proposed two degree-of-freedom GPC [16] in order to solve the above problem. For linear time invariant systems, its method has the ability to avoid the slow transient response or the extra control input because the integral compensation of two degree-of-freedom GPC emerges only when there is modeling error or disturbance.

In our research group, in order to keep a bipedal walking, the torques τ_5 and τ_6 to make floating-leg step forward are defined by trial and error as follows:

$$\tau_5 = 20\cos\{2\pi(t-t_1)/1.85\}, \tag{8}$$
$$\tau_6 = 100(-0.5-q_6). \tag{9}$$

Although the torque τ_5 is based on periodic function, human being does not make an effort to walk periodically. In other words, humans' periodic walking results in switching floating-leg and supporting-leg repeatedly.

Whereas, it seems that the concept to decide next motion from current state and prediction of future state is acceptable for human being. In other words, we believe that the merit of combination of GPC and VLS has a potential to realize humanoid's walking like human walking. Therefore this paper explores two degree-of-freedom GPC in order to make floating-leg step forward as a first step of humanoid's walking. In concrete terms, two degree-of-freedom GPC in this paper treats the floating-leg consisting of link-5 and link-6 as two-link arm, where the base joint is q_5. Equation of motion for the floating-leg (two-link arm) is linearized at $\tilde{q}_5$ and $\tilde{q}_6$. Then the state space equation is obtained as follows:

$$\boldsymbol{x}[k+1] = \boldsymbol{A}\boldsymbol{x}[k] + \boldsymbol{B}\boldsymbol{u}[k], \tag{10}$$
$$\boldsymbol{y}[k] = \boldsymbol{C}\boldsymbol{x}[k], \tag{11}$$

where the state $\boldsymbol{x}[k] = [q_5[k]\ q_6[k]\ \dot{q}_5[k]\ \dot{q}_6[k]]^{\mathrm{T}}$, the input $\boldsymbol{u}[k] = [\tau_5[k]\ \tau_6[k]]^{\mathrm{T}}$ and the output $\boldsymbol{y}[k] = [q_5[k]\ q_6[k]]^{\mathrm{T}}$, $\boldsymbol{A}$, $\boldsymbol{B}$ and $\boldsymbol{C}$ are system matrices with proper dimension. It is noticed that z^{-1} is shift operator $z^{-1}y[k] = y[k-1]$ and the above equation is assumed to be discretized at the same sampling time as simulation environment. An integrator $\boldsymbol{w}[k]$ is given by:

$$\boldsymbol{w}[k] = \frac{1}{\Delta}\boldsymbol{e}[k], \tag{12}$$

where $\Delta = 1 - z^{-1}$, and $\boldsymbol{e}[k] = \boldsymbol{r} - \boldsymbol{y}[k]$ is the following error between the reference signal $\boldsymbol{r} = [\tilde{q}_5\ \tilde{q}_6]$ and the output.

For the above system, the control law of two degree-of-freedom GPC [16] can be derived by minimization of a performance index containing $\boldsymbol{e}[k]$ and $\boldsymbol{u}[k]$.

$$\boldsymbol{u}[k] = \boldsymbol{F}_0\boldsymbol{x}[k] + \boldsymbol{H}_0\boldsymbol{r} + \boldsymbol{G}_0\boldsymbol{z}[k] \tag{13}$$

Where

$$\boldsymbol{z}[k] = \boldsymbol{w}[k] + \boldsymbol{C}(\boldsymbol{A}-\boldsymbol{I}+\boldsymbol{B}\boldsymbol{F}_0)^{-1}(\boldsymbol{A}+\boldsymbol{B}\boldsymbol{F}_0) \cdot(\boldsymbol{x}[k]-\boldsymbol{x}[0]), \tag{14}$$
$$\boldsymbol{H}_0 = -\left\{\boldsymbol{C}(\boldsymbol{A}-\boldsymbol{I}+\boldsymbol{B}\boldsymbol{F}_0)^{-1}\boldsymbol{B}\right\}^{-1}, \tag{15}$$
$$\boldsymbol{F}_0 = -[\boldsymbol{I}_m\ \boldsymbol{0}_m\ \cdots\ \boldsymbol{0}_m](\boldsymbol{G}^{\mathrm{T}}\boldsymbol{G}+\boldsymbol{\Lambda})^{-1}\boldsymbol{G}^{\mathrm{T}}\boldsymbol{H},$$
$$\boldsymbol{H} = \begin{bmatrix} \boldsymbol{C}\boldsymbol{A}^{N_1} \\ \boldsymbol{C}\boldsymbol{A}^{N_1+1} \\ \vdots \\ \boldsymbol{C}\boldsymbol{A}^{N_2} \end{bmatrix},\ \boldsymbol{\Lambda} = \begin{bmatrix} \boldsymbol{\Lambda}_1 & \boldsymbol{0} & \cdots & \boldsymbol{0} \\ \boldsymbol{0} & \boldsymbol{\Lambda}_2 & \ddots & \vdots \\ \vdots & \ddots & \ddots & \boldsymbol{0} \\ \boldsymbol{0} & \cdots & \boldsymbol{0} & \boldsymbol{\Lambda}_{N_u} \end{bmatrix},$$

$$\boldsymbol{G} = \begin{bmatrix} \boldsymbol{C}\boldsymbol{A}^{N_1-1}\boldsymbol{B} & \cdots & \boldsymbol{C}\boldsymbol{B} & \cdots & \boldsymbol{0} \\ \vdots & \ddots & \vdots & \ddots & \vdots \\ \boldsymbol{C}\boldsymbol{A}^{N_u-1}\boldsymbol{B} & \ddots & \ddots & \ddots & \boldsymbol{C}\boldsymbol{B} \\ \vdots & & \vdots & & \vdots \\ \boldsymbol{C}\boldsymbol{A}^{N_2-1}\boldsymbol{B} & \cdots & \cdots & \cdots & \boldsymbol{C}\boldsymbol{A}^{N_2-N_u}\boldsymbol{B} \end{bmatrix}.$$

$[N_1, N_2]$ is prediction horizon and $[1, N_u]$ is control horizon. In this paper, the prediction horizon is considered as the period of floating-leg stride. Combining two degree-of-freedom GPC expressed as Eq. (13) with VLS, the controller for walking is derived.

IV. Example of Bipedal Walking

Under the environment that sampling time was set as 3.0×10^{-3} [sec] and friction force between foot and the ground as $f_t = 0.7f_{n_z}$, the following simulations were conducted. In regard to simulation environment, we used "Borland C++ Builder Professional Ver. 5.0" to make simulation program and "OpenGL Ver. 1.5.0" to display humanoid's time-transient configurations.

In order to adopt two degree-of-freedom GPC for floating-leg, two-link arm model consisting of q_5 and q_6 is linearized at $\tilde{q}_5 = 0.7$ and $\tilde{q}_6 = -0.5$ and discretized with the same sampling time as the simulation environment of bipedal walking. Then the controlled system parameters are given as:

$$\boldsymbol{A} = \begin{bmatrix} 1.0001 & -0.0001 & 0.0029 & 0.0002 \\ -0.0000 & 1.0003 & 0.0002 & 0.0024 \\ 0.0606 & -0.0321 & 0.9539 & 0.0953 \\ -0.0258 & 0.1656 & 0.0953 & 0.6513 \end{bmatrix},$$
$$\boldsymbol{B} = \begin{bmatrix} 0.0000 & -0.0000 \\ -0.0000 & 0.0001 \\ 0.0046 & -0.0095 \\ -0.0095 & 0.0349 \end{bmatrix},\ \boldsymbol{C} = \begin{bmatrix} 1 & 0 & 0 & 0 \\ 0 & 1 & 0 & 0 \end{bmatrix}.$$

In this simulation the control parameters are set to be $[N_1, N_2] = [1, 250]$, $N_u = 250$ and $\boldsymbol{\Lambda}_i = \mathrm{diag}\{0.003, 0.005\}$ $(i = 1, \cdots, N_u)$. It is noticed that N_2 and N_u in the control parameters are considered as the period of floating-leg stride, that is, this simulation considers its period as 0.75 [sec]. Moreover, $\boldsymbol{\Lambda}_i$ is designed heuristically. Then the controller coefficients of two degree-of-freedom GPC Eq. (13) for τ_5 and τ_6 are derived as:

$$\boldsymbol{F}_0 = \begin{bmatrix} -40.0129 & -6.3938 & -4.4539 & -1.2532 \\ -4.2050 & -15.6389 & -0.9028 & -0.3517 \end{bmatrix},$$
$$\boldsymbol{H}_0 = \begin{bmatrix} 13.4014 & -0.1374 \\ -2.3262 & 9.1077 \end{bmatrix},$$

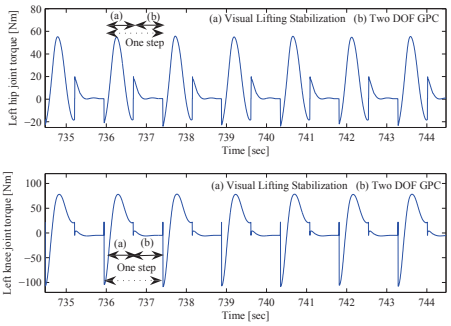

Fig. 7. Torques of left hip joint (upper) and left knee joint (lower)

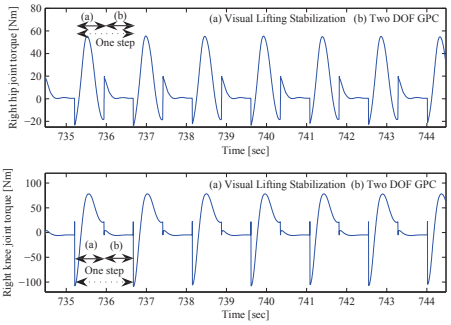

Fig. 8. Torques of right hip joint (upper) and right knee joint (lower)

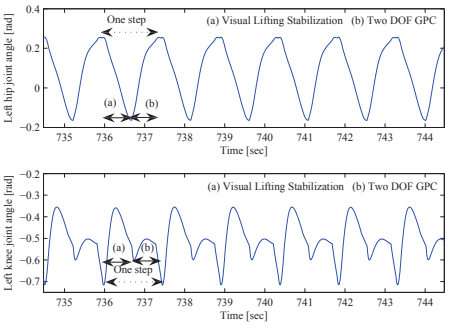

Fig. 9. Angles of left hip joint (upper) and left knee joint (lower)

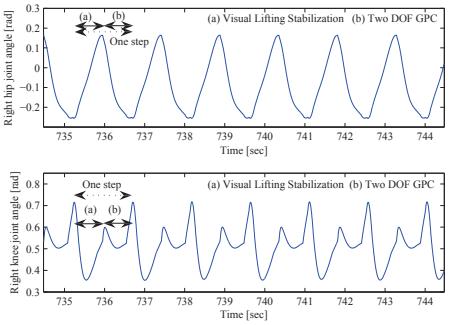

Fig. 10. Angles of right hip joint (upper) and right knee joint (lower)

where the integral gain $\boldsymbol{G}_0$ is chosen to be diag$\{0.05, 0.1\}$. The humanoid walked as shown in Fig. 6 and the followings are the results when the number of humanoid's walking steps is 5544: average length and period of floating-leg stride are 0.433 [m] and 0.735 [sec] respectively, and walking speed is 2.127 [km/h]. Figure 7 shows input torques for left hip and knee joints in about 10 seconds after 1001 steps, and Fig. 8 does for right hip and knee joints. And their figures show that each walking step includes the supporting-leg and the floating-leg states, in other words, each walking step strategy includes (a)VLS and (b)two degree-of-freedom GPC. Figure 9 shows joint angles of left hip and knee in about 10 seconds after 1001 steps, and Fig. 10 also shows them of right hip and knee. From these figures, it finds that the bipedal walking strategy proposed in this paper can help generate periodic walking motion. Figure 11 and 12 show motion trajectories of neck (origin of link-18 from waist (link-9)) in x-y and y-z planes respectively. And Fig. 13 and 14 depict the phase plane of q_{10} and $\dot{q}_{10}$. In each figure, its trajectory is depicted in about 10 seconds after 1001 steps. In Fig. 11 it is confirmed that motion concerning left and right side against $x = 0$ is almost symmetric, which means the neck and shoulder swung along with y-axis given at Fig. 11, representing rolling motion of upper body. In Fig. 12, the neck swayed in sagittal plane forward and backward with height varying by walking states including impact (contacting) state. Although limit cycle does not always emerge in Fig. 13 and 14, there was no turnover and walking motion was going on with gait transition during this simulation.

V. Conclusion

As a first step to realize human-like natural walking, this paper explores humanoid's walking by using two degree-of-freedom generalized predictive control (GPC) combined with visual lifting stabilization (VLS), based on strict dynamical model which contains flat feet including toe, slipping and impact. Two degree-of-freedom GPC and VLS are used for control of floating-leg and supporting-leg respectively, that is, two degree-of-freedom GPC makes floating-leg step forward and VLS compensates the falling motions caused by unpredictable slipping or unstable gaits. In the simulation results, we confirmed that the combined strategy could help realize a ZMP-independent stable walking. As future works, in order to verify the validity of the proposed method, noise and perturbation on the humanoid model are considered. Moreover there are a comparison with the other control approach such as optimal control and a validation through real bipedal robots.

VI. Acknowledgement

This work was supported by JSPS KAKENHI Grant Number 24760337 and Okayama Foundation for Science and Technology.

References

[1] S. Kajita, M. Morisawa, K, Miura, S. Nakaoka, K. Harada, K. Kaneko, F. Kanehiro and K. Yokoi, "Biped Walking Stabilization Based on Linear Inverted Pendulum Tracking," *Proceedings of IEEE/RSJ International Conference on Intelligent Robots and Systems*, pp.4489–4496, 2010.

[2] S. Kajita, F. Kanehiro, K. Kaneko, K. Yokoi and H. Hirukawa, "The 3D Linear Inverted Pendulum Mode: A simple modeling for a biped walking pattern generation," *Proceedings of IEEE/RSJ International Conference on Intelligent Robots and Systems*, 2001.

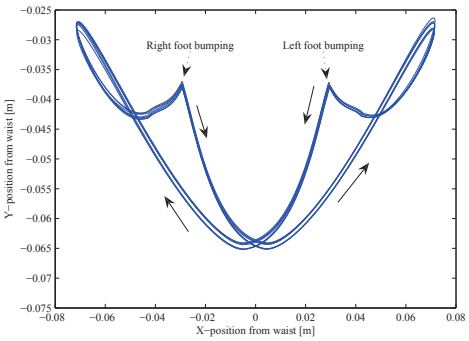

Fig. 11. X-Y motion trajectory of neck

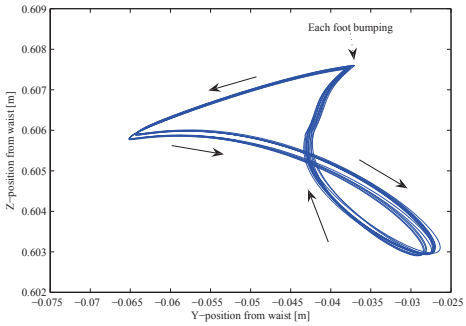

Fig. 12. Y-Z motion trajectory of neck

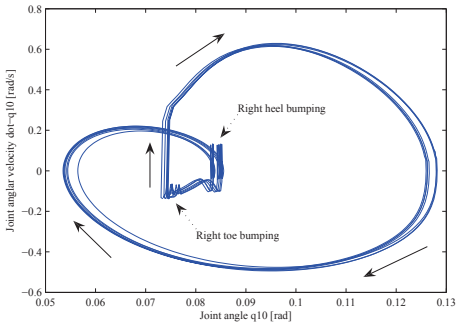

Fig. 13. q_{10} and $\dot{q}_{10}$ after 1001 steps in case of left supporting-leg

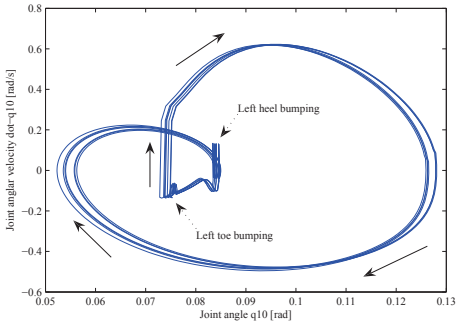

Fig. 14. q_{10} and $\dot{q}_{10}$ after 1001 steps in case of right supporting-leg

[3] J.H. Park and K.D. Kim, "Biped walking robot using gravity-compensated inverted pendulum mode and computed torque control," *Proceedings of IEEE International Conference on Robotics and Automation*, Vol.4, pp.3528–3593, 1998.

[4] P.B. Wieber, "Trajectory free linear model predictive control for stable walking in the presence of strong perturbations," *Proceedings of International Conference on Humanoid Robotics*, 2006.

[5] A. Herdt, N. Perrin and P.B. Wieber, "Walking without thinking about it," *Proceedings of IEEE/RSJ International Conference on Intelligent Robots and Systems*, pp.190–195, 2010.

[6] M. Vukobratovic, A. Frank and D. Juricic, "On the Stability of Biped Locomotion," *IEEE Transactions on Biomedical Engineering*, Vol.17, No.1, 1970.

[7] M. Vukobratovic and J. Stepanenko, "On the Stability of Anthropomorphic Systems," *Mathematical Biosciences*, Vol.15, pp.1–37, 1972.

[8] S. Colins, A. Ruina, R. Tedrake and M. Wisse, "Efficient Bipedal Robots Based on Passive-Dynamic Walkers," *Science*, Vol.307, pp.1082–1085, 2005.

[9] R.E. Westervelt, W.J. Grizzle and E.D. Koditschek, "Hybrid Zero Dynamics of Planar Biped Walkers," *IEEE Transactions on Automatic Control*, Vol.48, No.1, pp.42–56, 2003.

[10] Y. Harada, J. Takahashi, D. Nenchev and D. Sato, "Limit Cycle Based Walk of a Powered 7DOF 3D Biped with Flat Feet," *Proceedings of IEEE/RSJ International Conference on Intelligent Robots and Systems*, pp.3623–3628, 2010.

[11] Y. Huang, B. Chen, Q. Wang, K. Wei and L. Wang, "Energetic efficiency and stability of dynamic bipedal walking gaits with different step lengths," *Proceedings of IEEE/RSJ International Conference on Intelligent Robots and Systems*, pp.4077–4082, 2010.

[12] T. Wu, T. Yeh and B. Hsu, "Trajectory Planning of a One-Legged Robot Performing Stable Hop," *Proceedings of IEEE/RSJ International Conference on Intelligent Robots and Systems*, pp.4922–4927, 2010.

[13] Y. Nakamura and K. Yamane, "Dynamics of Kinematic Chains with Discontinuous Changes of Constraints—Application to Human Figures that Move in Contact with the Environments—," *Journal of RSJ*, Vol.18, No.3, pp.435–443, 2000 (in Japanese).

[14] W. Song, M. Minami, T. Maeba, Y. Zhang and A. Yanou, "Visual Lifting Stabilization of Dynamic Bipedal Walking," *Proceedings of 2011 IEEE-RAS International Conference on Humanoid Robots*, pp.345–351, 2011.

[15] N. Hogan, "Impedance Control; An Approach to Manipulation, Parts I–III, *ASME Journal of Dynamics Systems, Measurement, and Control* Vol.107, No.1, pp.1–24, 1985.

[16] A. Yanou, S. Masuda and A. Inoue, "Two Degree-of-Freedom of Generalized Predictive Control for m-input m-output Systems Based on State Space Approach," *Proc. of SICE Annual Conference 2004 in Sapporo*, pp.2680–2684, 2004.

[17] M. Kouchi, M. Mochimaru, H. Iwasawa and S. Mitani, "Anthropometric database for Japanese Population 1997-98," Japanese Industrial Standards Center (AIST, MITI), 2000.

[18] Y. Fujimoto and A. Kawamura, "Three Dimensional Digital Simulation and Autonomous Walking Control for Eight-Axis Biped Robot," *Proceedings of IEEE International Conference on Robotics and Automation*, pp.2877–2884, 1995.

[19] J.Y.S. Luh, M.W. Walker and R.P.C. Paul, "On-Line Computational Scheme for Mechanical Manipulators," *ASME Journal of Dynamics Systems, Measurement, and Control*, Vol.102, No.2, pp.69–76, 1980.

[20] W. Song, M. Minami, F. Yu, Y. Zhang and A. Yanou, "3-D Hand & Eye-Vergence Approaching Visual Servoing with Lyapunov-Stable Pose Tracking," *Proceedings of IEEE International Conference on Robotics and Automation*, pp.5210–5217, 2011.

[21] T. Maeba, M. Minami, A. Yanou, T. Matsuno and J. Nishiguchi, "Dynamical Analyses of Humanoidfs Walking by Visual Lifting Stabilization Based on Event-driven State Transition," *Proceedings of the 2012 IEEE/ASME International Conference on Advanced Intelligent Mechatronics*, pp.7–14, 2012.

[22] D. W. Clarke, C. Mohtadi and P. S. Tuffs, "Generalized Predictive Control," *Automatica*, Vol.23, No.2, pp.137–160, 1987.